Cyanide-bridged 1D Mn(III)–Fe(III) bimetallic complexes: synthesis, crystal structure and magnetic properties†

Hui-Zhong Kou,*[a] Zhong-Hai Ni,[a] Cai-Ming Liu,[b] De-Qing Zhang[b] and Ai-Li Cui[a]

Received (in Montpellier, France) 7th July 2009, Accepted 24th August 2009
First published as an Advance Article on the web 22nd September 2009
DOI: 10.1039/b9nj00316a

Cyanide-bridged Mn(III)–Fe(III) complexes have been synthesized in order to find new molecular materials with interesting magnetic properties. 1D complexes of *trans*-dicyanoferrite(III), $[Mn(5\text{-Cl-salen})Fe(bpClb)(CN)_2]\cdot 0.67MeCN\cdot 0.5H_2O$ (**1**), $[Mn(5\text{-Cl-salen})Fe(bpb)(CN)_2]\cdot 0.5H_2O\cdot MeOH$ (**2**), $[Mn(5\text{-Br-salen})Fe(bpb)(CN)_2]\cdot 0.5H_2O\cdot MeOH$ (**3**), and $[Mn(5\text{-Me-salen})Fe(bpb)(CN)_2]\cdot 0.5H_2O\cdot MeOH$ (**4**) have been prepared and characterized by X-ray single-crystal structure analysis and magnetic measurements. All complexes possesses 1D chains of alternate $[Mn(5\text{-R-salen})]^+$ and $[Fe(bpRb)(CN)_2]^-$ units that are linked by two *trans*-cyanide ligands of $[Fe(bpRb)(CN)_2]^-$. Magnetic studies reveal that they exhibit overall intermetallic ferromagnetic coupling, while complex **4** shows a frequency-dependent AC magnetic susceptibility typical of a single-chain magnet.

Introduction

In the field of molecule-based magnets, the rational design of single-chain magnets has aroused widespread concern.[1] Such materials are still few because of the difficulty of controlling the construction of their 1D structure and magnetic coupling. Some cyanide-bridged 1D bimetallic compounds have been obtained, mainly based on $[M(L)(CN)_x]^{n-}$ (L is an aza ligand; $x = 2, 3, 4, 5$; $n = 1, 2$).[2,3] This hybrid approach (by the inclusion of L) provides an interesting way, for instance, of constructing low-dimensional magnetic materials, single-molecule magnets (SMMs) and single-chain magnets (SCMs).[3]

Mn(III) Schiff bases $[M(SB)]^+$ have been widely used for the synthesis of low-dimensional magnets, because Mn(III) meets the requirement of uniaxial anisotropy (negative *D*) for SMMs or SCMs.[4] We recently initialized a study on cyanide-bridged Mn(III)–Fe(III) complexes based on *trans*-$[Fe(III)(L)(CN)_2]^-$ building blocks (L^{2-} = bpmb, bpClb or bpdmb, as shown in Scheme 1),[5–10] and found that large cyclic dodecanuclear complexes can be isolated that display SMM behavior.[6]

1D cyanide-bridged Fe(III)–Mn(III) complexes based on $[Mn(SB)(H_2O)_2]^+$ and *trans*-$[Fe(III)(L)(CN)_2]^-$ building blocks are expected, from which single-chain magnets may be found. Herein, we report the characterization and magnetic properties of four 1D complexes $[Mn(5\text{-Cl-salen})Fe(bpClb)(CN)_2]\cdot 0.67MeCN\cdot 0.5H_2O$ (**1**), $[Mn(5\text{-Cl-salen})Fe(bpb)(CN)_2]\cdot 0.5H_2O\cdot MeOH$ (**2**), $[Mn(5\text{-Br-salen})Fe(bpb)(CN)_2]\cdot 0.5H_2O\cdot MeOH$ (**3**) and $[Mn(5\text{-Me-salen})Fe(bpb)(CN)_2]\cdot 0.5H_2O\cdot MeOH$ (**4**).

Experimental

Materials

All chemicals were of AR grade and used as received. $K[Fe(bpRb)(CN)_2]$[10–12] and $[Mn(5\text{-X-salen})]ClO_4$[13] were synthesized according to literature methods.

Physical measurements

Elemental analyses (C, H, N) were carried out using an Elementar Vario EL analyzer. IR spectra were recorded on a Nicolet Magna-IR 750 spectrometer in the 4000–650 cm^{-1} region. Temperature- and field-dependent magnetic susceptibility measurements were carried out on a Quantum Design SQUID magnetometer. Alternating current (AC) magnetic susceptibility measurements were performed on a MagLab 2000 magnetometer. Experimental susceptibilities were corrected for the diamagnetism of the constituent atoms (Pascal's tables).

Single-crystal X-ray data of **1–4** were collected on a Rigaku R-AXIS RAPID IP or a Saturn70 CCD diffractometer. The

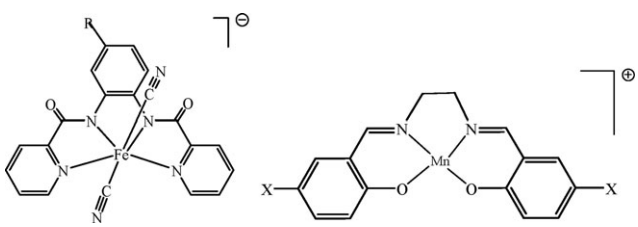

Scheme 1 The structures of building blocks $[Fe(III)(bpRb)(CN)_2]^-$ ($bpRb^{2-}$ = bpb^{2-} (R = H), $bpClb^{2-}$ (R = Cl)) and $[Mn(III)(5\text{-X-salen})]^+$ (5-X-salen = 5-Cl-$salen^{2-}$ (X = Cl), 5-Br-$salen^{2-}$ (X = Br), 5-Me-$salen^{2-}$ (X = Me)).

[a] *Department of Chemistry, Tsinghua University, Beijing 100084, P. R. China. E-mail: kouhz@mail.tsinghua.edu.cn; Fax: +86 10-62771748*
[b] *Beijing National Laboratory for Molecular Sciences, Center for Molecular Science, Institute of Chemistry, Chinese Academy of Sciences, Beijing 100080, P. R. China*

† Electronic supplementary information (ESI) available: CCDC 744627–744630. Cell packing diagrams for complexes **1** and **2**. Temperature dependence of in-phase ac magnetic susceptibility for complex **4**. For ESI and crystallographic data in CIF or other electronic format see DOI: 10.1039/b9nj00316a

structures were solved by direct methods SHELXS-97 and refined by full-matrix least-squares (SHELXL-97) on F^2. Hydrogen atoms were added geometrically and refined using a riding model.

Synthesis

[Mn(5-Cl-salen)Fe(bpClb)(CN)$_2$]·0.67MeCN·0.5H$_2$O (1), [Mn(5-Cl-salen)Fe(bpb)(CN)$_2$]·0.5H$_2$O·MeOH (2), [Mn(5-Br-salen)Fe(bpb)(CN)$_2$]·0.5H$_2$O·MeOH (3) and [Mn(5-Me-salen)-Fe(bpb)(CN)$_2$]·0.5H$_2$O·MeOH (4). At room temperature, a methanol/water solution (5 mL, methanol/water = 4 : 1) of *trans*-K[Fe(L)(CN)$_2$]] (0.15 mmol) was added to a methanol/acetonitrile (6 mL, methanol/acetonitrile = 2 : 1) solution of the corresponding [Mn(SB)]ClO$_4$ (0.15 mmol). Slow evaporation of the resultant solution gave red-brown single-crystals after one week.

Elemental analysis for complex **1**: calc. for FeMnC$_{37.35}$H$_{26.01}$Cl$_3$N$_{8.67}$O$_{4.5}$: C, 50.67; H, 2.96; N, 13.72. Found: C, 50.59; H, 3.43; N 14.09%. IR (KBr/cm^{-1}): 2122, 2129. Yield: 50%.

Elemental analysis for complex **2**: calc. for FeMnC$_{37}$H$_{29}$Cl$_2$N$_8$O$_{5.5}$: C, 51.95; H, 3.42; N, 13.10. Found: C, 51.36; H, 3.48; N, 12.95%. IR (KBr/cm^{-1}): 2122, 2129. Yield: 50%.

Elemental analysis for complex **3**: calc. for FeMnC$_{37}$H$_{29}$Br$_2$N$_8$O$_{5.50}$: C, 47.06; H, 3.10; N, 11.87. Found: C, 46.74; H, 3.27; N, 11.62%. IR (KBr/cm^{-1}): 2121, 2127. Yield: 60%.

Elemental analysis for complex **4**: calc. for FeMnC$_{39}$H$_{35}$N$_8$O$_{5.50}$: C, 57.51; H, 4.33; N, 13.76. Found: C, 57.26; H, 4.28; N, 13.76%. IR (KBr/cm^{-1}): 2121, 2128. Yield: 60%.

Results and discussion

Structural descriptions

The crystal data and structure refinement details for compounds **1–4** are listed in Table 1. Selected bond lengths and angles are collected in Table 2. Representative structural diagrams of complexes **1–4** are shown in Fig. 1, while cell packing diagrams are given in the ESI.†

X-Ray diffraction structure analyses shows that the complexes have a chain structure consisting of alternate Fe(III) and Mn(III) ions. In the chains, each *trans*-[Fe(L)(CN)$_2$]$^-$ connects two *trans*-[Mn(SB)]$^+$ with two *trans*-cyanide groups, and in turn each *trans*-[Mn(SB)]$^+$ unit links two *trans*-[Fe(L)(CN)$_2$]$^-$ building blocks. In the chains of complexes **2–4**, the [Fe(bpb)(CN)$_2$]$^-$ moieties arrange themselves in an up–down fashion. In complex **1**, the [Fe(bpClb)(CN)$_2$]$^-$ groups are disposed parallel to each other in a chain, different to complexes **2–4** (Fig. 1 and ESI†).

The coordination configuration of the Fe(III) in complexes **1–4** is similar, with Fe–C bond lengths in the range 1.939(8)–2.002(3) Å and Fe–C≡N bond angles in the range 172.4(4)–177.0(3)°. However, the Mn(III) coordination environments are somewhat different; the Mn–N$_{cyano}$ bonds are their shortest (<2.28 Å) in complex **1**, and complexes **3** and **4** possess the longest Mn–N$_{cyano}$ bonds (>2.3 Å). The long coordination of the cyanide nitrogen atoms gives rise to an elongated octahedral geometry around the Mn(III), with the Jahn–Teller axis lying along the *z* direction, *i.e.* the N$_{cyano}$–Mn–N′$_{cyano}$ axis. The bridging Mn–N≡C bond angles lie in the small range 147.5(3)–161.0(3)°. These data are comparable with related complexes previously reported.[5,6,9]

In the unit cell, the zig-zag chains extend along the *a* axis for complex **1** and along the *c* axis for complexes **2–4**. The nearest interchain metal–metal separations are in the range 7.108–8.119 Å for Mn–Mn′. Although close, no apparent supramolecular interactions are present between the related [Mn(SB)]$^+$ groups. Similar to other [Fe(bpb)(CN)$_2$]$^-$-based complexes, the benzene group of the bpb^{2-} of adjacent chains is involved in a π–π interaction in complexes **2–4**.[9] However, for [Fe(bpClb)(CN)$_2$]$^-$ in complex **1**, the presence of the Cl substituent in bpClb^{2-} precludes the formation of the π–π interaction because of steric hindrance.

Magnetic properties

The variable-temperature magnetic susceptibilities of complexes **1–4** have been measured on a SQUID magnetometer in the

Table 1 Crystallographic data for complexes **1–4**

	1	2	3	4
Formula	FeMnC$_{37.35}$H$_{26.01}$Cl$_3$N$_{8.67}$O$_{4.5}$	FeMnC$_{37}$H$_{29}$Cl$_2$N$_8$O$_{5.5}$	FeMnC$_{37}$H$_{29}$Br$_2$N$_8$O$_{5.50}$	FeMnC$_{39}$H$_{35}$N$_8$O$_{5.50}$
M_w	885.37	855.37	944.29	814.54
Crystal system	Monoclinic	Triclinic	Triclinic	Triclinic
Space group	*P*2/*c*	*P*-1	*P*-1	*P*-1
a/Å	10.267(5)	11.013(2)	11.1567(9)	11.2920(13)
b/Å	13.751(6)	15.613(3)	15.4314(13)	15.4950(17)
c/Å	29.045(13)	20.586(4)	20.8618(17)	20.801(3)
α (°)	90	91.74(3)	91.765(2)	92.693(7)
β (°)	95.637(3)	92.56(3)	92.646(2)	93.138(6)
γ (°)	90	90.89(3)	91.871(2)	92.0650(13)
V/Å^3	4081(3)	3534.0(12)	3584.0(5)	3627.3(7)
Z	4	*4*	4	4
ρ_{calc}/g cm^{-3}	1.441	1.608	1.750	1.492
μ/mm^{-1}	0.912	0.979	3.046	0.807
Observed data [$I > 2\sigma(I)$]	6310	8743	13210	12679
GOF	1.079	*1.133*	1.059	1.020
*R*1[$I > 2\sigma(I)$]	0.0775	0.1031	0.0499	0.0700
w*R*2 (all data)	0.2284	0.3260	0.1214	0.1925
CCDC number	744627	744628	744629	744630

Table 2 Selected bond lengths (Å) and bond angles (°) for complexes **1–4**

	1	2	3	4
Mn–N_{salen}	2.003(4)–2.008(4)	1.986(7)–2.022(7)	1.989(3)–1.998(3)	2.016(3)–2.028(3)
Mn–O	1.885(3)–1.906(3)	1.859(6)–1.903(6)	1.868(2)–1.889(2)	1.883(3)–1.910(2)
Mn–N_{cyano}	2.258(4)–2.277(4)	2.270(7)–2.339(7)	2.304(3)–2.372(3)	2.308(3)–2.376(3)
Fe–C	1.947(5)–1.955(5)	1.939(8)–1.958(8)	1.960(3)–1.989(3)	1.980(3)–2.002(3)
Fe–$N_{pyridine}$	1.994(4)–1.996(4)	1.961(7)–2.026(7)	1.987(2)–2.006(2)	1.992(3)–2.028(3)
Fe–N_{amide}	1.886(4)–1.889(4)	1.876(6)–1.898(6)	1.882(2)–1.899(2)	1.888(3)–1.930(3)
Mn–N≡C	149.5(4)–154.3(3)	149.1(7)–160.8(7)	149.0(3)–161.3(2)	147.5(2)–160.9(3)
Fe–C≡N	172.5(4)–172.7(4)	172.8(7)–176.8(8)	172.5(3)–175.9(3)	171.4(3)–177.0(3)
Fe–Mn[a]	5.119(1), 5.175(1)	5.128(2), 5.183(2)	5.182(1), 5.256(1)	5.210(1), 5.205(1)
		5.132(2), 5.349(2)	5.210(1), 5.414(1)	5.176(1), 5.444(1)
M–M′[b]	7.108 (Mn–Mn″)	7.787 (Mn–Mn″)	7.678 (Mn–Mn)	8.119 (Mn–Mn′)

[a] Adjacent intermetallic separations through the cyanide bridges. [b] Interchain metal–metal separations.

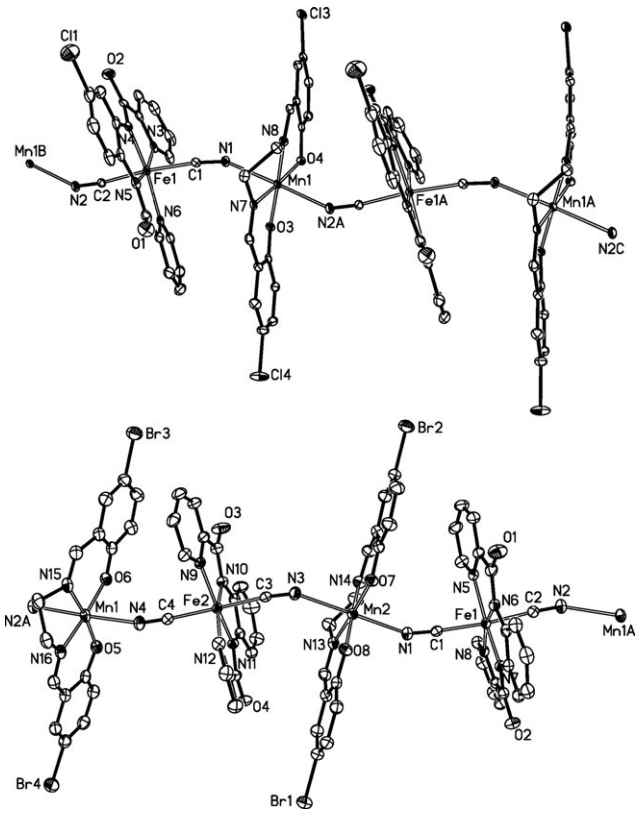

Fig. 1 View of the zig-zag chain for complex **1** (top) and **3** (bottom) (30% probability ellipsoids). Hydrogen atoms are omitted for clarity. Symmetry codes for complex **1** A: $1 + x, y, z$; B: $-1 + x, y, z$; C: $1 + x, y, z$. Symmetry codes for complex **3** A: $x, y, -1 + z$; B $x, y, 1 + z$.

temperature range 2–300 K. Fig. 2 shows the $\chi_m T$ *vs.* T plots for complexes **1–4**, respectively.

The magnetic properties of complexes **1–4** are similar. The $\chi_m T$ values per MnFe at room temperature are in the range 3.34–3.59 emu K mol^{-1}, which is close to the spin-only value of 3.375 emu K mol^{-1} ($g = 2.0$) for non-coupling low-spin Fe(III) and high-spin Mn(III). The $\chi_m T$ increases with decreasing temperature, then decreases at lower temperatures. From the plots, the Weiss constant and Curie constant can be obtained based on the Curie–Weiss law $\chi = C/(T - \theta)$ (Table 3). Therefore, the variable-temperature magnetic susceptibility data for complexes **1–4** show that the overall magnetic coupling between adjacent Mn(III) and Fe(III) is ferromagnetic.

Because of the presence of different bridging angles in the MnFe chain for complexes **1–4**, the two-J model was used to reproduce the experimental magnetic susceptibility. The MAGPACK program[14] was used based on the Hamiltonian $H = -2J_1(S_{Mn1}S_{Fe1} + S_{Mn2}S_{Fe2} + S_{Mn3}S_{Fe3} + S_{Mn4}S_{Fe4}) - 2J_2(S_{Fe1}S_{Mn2} + S_{Fe2}S_{Mn3} + S_{Fe3}S_{Mn4} + S_{Fe4}S_{Mn1})$ for the Mn_4Fe_4 ring shown in Scheme 2. The fit to the experimental magnetic data (20–300 K) gave the parameters shown in Table 3. More accurately, the Mn_5Fe_5 ring (Scheme 2) can be used; however, identical fit results were obtained. This shows that it is appropriate to use the Mn_4Fe_4 model to reproduce the magnetic susceptibility of the 1D chain complexes. Unexpectedly, alternate intrachain ferromagnetic (J_1) and antiferromagnetic (J_2) coupling was found in complexes **1–3**, different from complex **4**, where a ferromagnetic interaction was found within the chain. Previously, we have found that for cyanide-bridged Mn(III)–Fe(III) complexes, C≡N–Mn bond angles below 162° most probably exhibit a ferromagnetic interaction, with few exceptions, and above 162° both ferromagnetic and antiferromagnetic properties are possible.[9] According to this assumption, complexes **1–4**, with Mn–N≡C bond angles of 147.5(3)–161.0(3)°, should most probably display a ferromagnetic interaction between adjacent metal ions. However, the fitting results are inconsistent with this assumption, indicating the complexity of the Fe(III)–Mn(III) magnetic coupling. This is because of the presence of ferromagnetic (σ–π magnetic orbital orthogonality) and antiferromagnetic (π–π magnetic orbital overlap) contributions.

AC magnetic susceptibility measurements for complex **4** were performed in a 3 G AC field oscillating at 111–9999 Hz, with a zero DC magnetic field, on polycrystalline samples (Fig. 3). Complex **4** exhibited obvious frequency-dependent χ_m'' signals at $T < 5$ K, suggesting the presence of slow relaxation of the magnetization. This indicates that the chain complex shows possible single-chain magnetic behaviour.[3] From the crystal data (Table 2), complex **4** has the longest interchain metal–metal separation among complexes **1–4**, yielding the weakest interchain magnetic interaction. Therefore, single-chain magnetic behaviour can be observed in complex **4**.

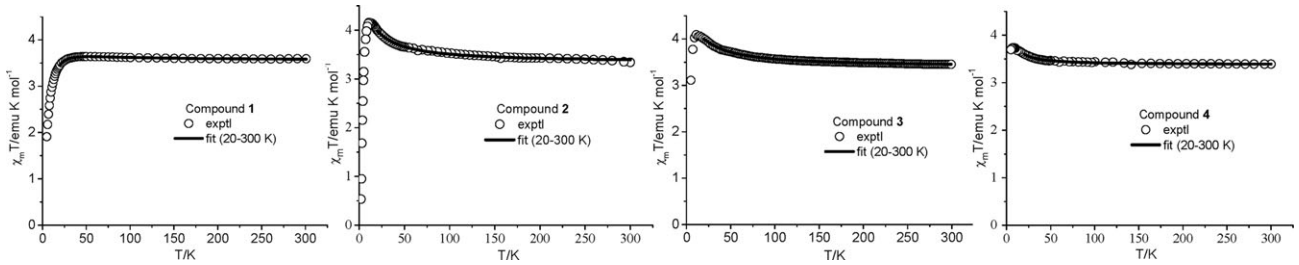

Fig. 2 The temperature dependence of $\chi_m T$ per MnFe for complexes **1–4**. The line represents the best fit (20–300 K) using the parameters discussed in the text.

Table 3 Magnetic data for complexes **1–4**

	1	2	3	4
θ/K	+0.45	+3.93	+4.20	+1.13
C/emu K mol^{-1}	3.58	3.35	3.41	3.38
g	2.05	1.99	2.01	2.00
J_1	3.61	4.30	4.46	0.49
J_2	−1.68	−0.080	−0.24	0.49

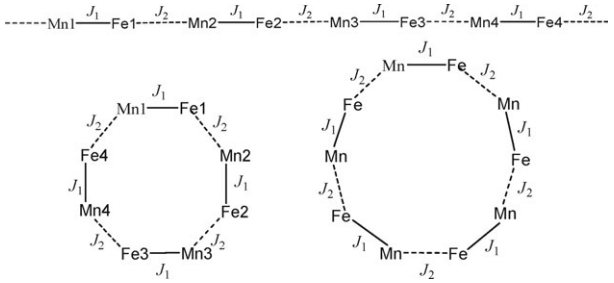

Scheme 2 The two-J model to fit the magnetic susceptibility of 1D complexes **1–4**.

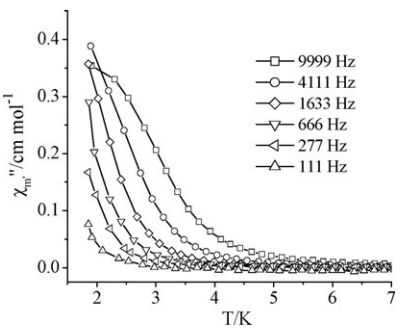

Fig. 3 Temperature-dependence of the AC magnetic susceptibility at different frequencies for complex **4**.

Acknowledgements

This work was supported by the Natural Science Foundation of China (project no. 20771065 and 50873053) and the Program for New Century Excellent Talents in University.

Notes and references

1 C. Coulon, H. Miyasaka and R. Clerac, *Struct. Bonding*, 2006, **122**, 163.
2 R. Lescouezec, L. M. Toma, J. Vaissermann, M. Verdaguer, F. S. Delgado, C. Ruiz-Perez, F. Lloret and M. Julve, *Coord. Chem. Rev.*, 2005, **249**, 2691; F. Pan, Z.-M. Wang and S. Gao, *Inorg. Chem.*, 2007, **46**, 10221; J. H. Yoon, H. S. Yoo, H. C. Kim, S. W. Yoon, B. J. Suh and C. S. Hong, *Inorg. Chem.*, 2009, **48**, 816; J. I. Kim, H. S. Yoo, E. K. Koh and C. S. Hong, *Inorg. Chem.*, 2007, **46**, 10461; L. M. Toma, L. D. Toma, F. S. Delgado, C. Ruiz-Perez, J. Sletten, J. Canod, J. M. Clemente-Juan, F. Lloret and M. Julve, *Coord. Chem. Rev.*, 2006, **250**, 2176; D. Zhang, H. Wang, Y. Chen, Z.-H. Ni, L. Tian and J. Jiang, *Inorg. Chem.*, 2009, **48**, 5488; W.-W. Ni, Z.-H. Ni, A.-L. Cui, X. Liang and H.-Z. Kou, *Inorg. Chem.*, 2007, **46**, 22.
3 J. I. Kim, H. S. Yoo, E. K. Koh, H. C. Kim and C. S. Hong, *Inorg. Chem.*, 2007, **46**, 8481; J. I. Kim, H. Y. Kwak, J. H. Yoon, D. W. Ryu, I. Y. Yoo, N. Yang, B. K. Cho, J.-G. Park, H. Lee and C. S. Hong, *Inorg. Chem.*, 2009, **48**, 2956; H.-R. Wen, C.-F. Wang, Y. Song, S. Gao, J.-L. Zuo and X.-Z. You, *Inorg. Chem.*, 2006, **45**, 8942; L. M. Toma, R. Lescouezec, F. Lloret, M. Julve, J. Vaissermann and M. Verdaguer, *Chem. Commun.*, 2003, 1850; S. Wang, J.-L. Zuo, S. Gao, Y. Song, H.-C. Zhou, Y.-Z. Zhang and X.-Z. You, *J. Am. Chem. Soc.*, 2004, **126**, 8900; H.-R. Wen, C.-F. Wang, Y.-Z. Li, J.-L. Zuo, Y. Song and X.-Z. You, *Inorg. Chem.*, 2006, **45**, 7032.
4 H. Miyasaka, A. Saitoh and S. Abe, *Coord. Chem. Rev.*, 2007, **251**, 2622.
5 Z.-H. Ni, H.-Z. Kou, L.-F. Zhang, C. Ge, A.-L. Cui, R.-J. Wang, Y. Li and O. Sato, *Angew. Chem., Int. Ed.*, 2005, **44**, 7742.
6 Z.-H. Ni, L.-F. Zhang, V. Tangoulis, W. Wernsdorfer, A.-L. Cui, O. Sato and H.-Z. Kou, *Inorg. Chem.*, 2007, **46**, 6029.
7 B. Zhang, Z.-H. Ni, A.-L. Cui and H.-Z. Kou, *New J. Chem.*, 2006, **30**, 1327.
8 Z.-H. Ni, H.-Z. Kou, Y.-H. Zhao, L. Zheng, R.-J. Wang, A.-L. Cui and O. Sato, *Inorg. Chem.*, 2005, **44**, 2050.
9 Z.-H. Ni, J. Tao, W. Wernsdorfer, A.-L. Cui and H.-Z. Kou, *Dalton Trans.*, 2009, 2788.
10 Z.-H. Ni, L.-F. Zhang, A.-L. Cui and H.-Z. Kou, *Sci. China, Ser. B: Chem.*, 2009, **52**, 1444.
11 D. J. Barnes, R. L. Chapman, R. S. Vagg and E. C. Watton, *J. Chem. Eng. Data*, 1978, **23**, 349.
12 (*a*) M. Ray, R. Mukherjee, J. F. Richardson and R. M. Buchanan, *J. Chem. Soc., Dalton Trans.*, 1993, 2451–2457; (*b*) S. K. Dutta, U. Beckmann, E. Bill, T. Weyhermuller and K. Wieghardt, *Inorg. Chem.*, 2000, **39**, 3355.
13 Z.-H. Ni, L. Zheng, L.-F. Zhang, A.-L. Cui, W.-W. Ni, C.-C. Zhao and H.-Z. Kou, *Eur. J. Inorg. Chem.*, 2007, 1240; P. Przychodzeń, K. Lewinski, M. Balanda, R. Pełka, M. Rams, T. Wasiutynshi, C. Guyard-Duhayon and B. Sieklucka, *Inorg. Chem.*, 2004, **43**, 2967.
14 J. J. Borrás-Almenar, J. M. Clemente-Juan, E. Coronado and B. S. Tsukerblat, *J. Comput. Chem.*, 2001, **22**, 985.